



VHE Gamma Ray Observations of Pulsars with HAGAR Telescope Array

B.B. SINGH¹, B.S. ACHARYA¹, V.R. CHITNIS¹, R.J. BRITTO¹, P.R. VISHWANATH², T.P. PRABHU², G.C. ANUPAMA², A. SHUKLA², P. BHATTACHARJEE³, L. SAHA³

¹Tata Institute of Fundamental Research, Mumbai, India

²Indian Institute of Astrophysics, Bangalore, India

³Saha Institute of Nuclear Physics, Kolkata, India

contact.person: bbsingh@tifr.res.in

DOI: 10.7529/ICRC2011/V07/0276

Abstract: We have searched for pulsed emission of VHE gamma rays from Crab, Geminga and 3 other pulsars from Fermi-LAT pulsar catalog. The observations were carried out using HAGAR telescope array which is a non-imaging wavefront sampling telescope array located at high altitude in the Himalayas. Crab and Geminga pulsars have been observed for more than 100 and 75 hours respectively since the commissioning phase of HAGAR. We have selected 3 pulsars from Fermi-LAT pulsar catalog, those pulsars with high-confidence pulsed emission, rotational energy loss rate and flat emission spectrum and accessible to the latitude of HAGAR for observations. Preliminary analysis indicate that there is no evidence of pulsed emission from any of these sources in our data at energies ≥ 200 GeV. In this work we report on our analysis techniques for the search of gamma ray emission in pulsed mode and set upper limits for the time averaged flux of gamma rays from these sources.

Keywords: Pulsars, VHE γ -ray, Atmospheric Cherenkov Detection

1 Introduction

Pulsars are highly magnetized, rotating neutron stars that emit a beam of electromagnetic radiation. The radiation can only be observed when the beam of emission is pointing towards the Earth. Any mis-alignment between the magnetic axis and the rotation axis of the pulsar results in pulsed nature of observed signal. In most cases the interval between observed pulses is very regular and their periods range from milliseconds to seconds. Pulsars have been classified into 3 distinct classes based on their sources for powering the electro-magnetic radiation, viz., Rotation-powered pulsars, where the loss of rotational energy of the star provides the power, Accretion-powered pulsars, where the gravitational potential energy of accreted matter is the power source and Magnetars, where the decay of an extremely strong magnetic field provides the electromagnetic power. Since the discovery of pulsars by Bell & Hewish [1] more than 1800 rotation-powered pulsars are now listed in the ATNF pulsar catalog [2]. The majority of these pulsars were discovered by radio telescopes, small number of pulsars also have been seen in the optical band, with more in the X-ray bands. Recently γ -ray alone pulsars have also been discovered using the Fermi-lat detector [3].

Radiation mechanism for pulsed emission, which of magnetospheric origin are explained with two models. In Polar cap model [4] particle acceleration take place near the neutron star magnetic poles. The charged particles (e^\pm) are

accelerated by strong fields and relativistic e^\pm emit gamma rays via synchrotron, curvature, and Inverse Compton (IC) processes. In this process, magnetic pair production dominate near polar region and sharp cutoff in γ -ray energy spectrum at a few GeV is expected. In the Outergap model [5, 6] the γ -rays are produced near the light cylinder via synchro-curvature radiation. In this case the effective magnetic field near light cylinder is small, and cutoff due to magnetic pair production is gentler than polar cap and γ -rays of higher energy (> 1 TeV) could be expected. A modern approach for γ -ray emission process is Slot Gap model [7], in which particle acceleration is along the edge of the open field region from the neutron star surface to near the light cylinder.

1.1 Gamma Ray Pulsar Search

In the high energy gamma ray domain (≥ 30 MeV), the first indications for pulsed emission were obtained for the Crab pulsar by balloon-borne detectors and later confirmed by the satellite based detectors SAS-II and COS-B. The detectors on board the Compton Gamma Ray Observatory (CGRO) expanded the number of gamma ray pulsars from two to seven. The Large Area telescope (LAT) on the Fermi Gamma Ray Telescope launched on 2008 June 11 has provided a major increase in the known gamma-ray pulsar population. This new detection has given a new class of (radio quiet but gamma ray loud) GeV gamma-ray pulsars.

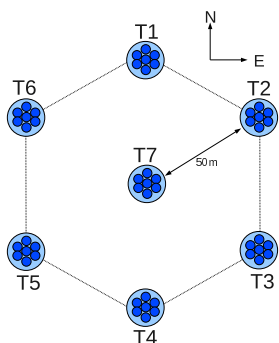


Figure 1: Schematic diagram of HAGAR array

Fermi-LAT detector has reported more than 54 pulsars including Crab and Geminga [3].

GeV-TeV photons are detected by ground based atmospheric Cherenkov telescopes. These telescopes detect faint flashes of Cherenkov light produced when gamma-rays (or cosmic rays) enter into the earth atmosphere and initiate showers of secondary particles. The Cherenkov light emitted by the charged secondary particles is reflected by the telescope mirror and recorded by fast photomultiplier tubes. In ground based detection, MAGIC telescope [9] has detected pulsed gamma-rays from the Crab pulsar at energies ≥ 25 GeV in VHE domain.

2 HAGAR

The High Altitude GAMMA Ray Observatory consists of an array of seven atmospheric Cherenkov telescopes located at the centre and corners of a hexagon inscribed in circle of 50 meter radius (figure-1). Each telescope consists of seven parabolic glass mirrors of 10 mm thickness and 0.9 m diameter having $f/d=1$. These mirrors are front coated and average reflectivity in the visible range is 70 %. Each mirror has a UV-blue sensitive XP2268B Photo-multiplier tube (PMT), mounted at its focal point with 3.0 deg of angular mask. The total reflector area is about 31 m². These telescopes which are based on Alt-Azimuth mounting are controlled remotely through Linux based system using 17-bit rotatory encoders, stepper motors, Microcontroller-based Motion control interface units (MCIU) etc. The control system allows to achieve a steady state pointing accuracy of 10 arcsec with maximum slew rate of 30 deg per minute for each axis and continuous monitoring of the telescope positions. Guide telescopes are used to arrive at a pointing model for each telescope. The co-planarity of all 7 mirrors of a given telescope with its axis is achieved by a series of bright star scans. The over-all accuracy in pointing of the mirrors is about 12 arc minutes [10]. The High Voltages to PMT's are controlled and monitored through CAEN universal multi-channel power supply system. The analog PMT signals are transmitted to the central control room located at the centre of the array (below Tel #7) through co-

Table 1: Observation log of sources.

Source	Observation period	Duration (h)
Crab	Oct 2008 - Jan 2011	119.6
Geminga	Dec 2008 - Jan 2011	81.3
PSR J0357+3206	Nov 2010	3.6
PSR J0633+0632	Dec 2010 - Jan 2011	14.1
PSR J2055+2539	Oct 2010 - Nov 2010	5.9

axial cables. A CAMAC based data acquisition system has been used for signal processing. An eight channel Flash ADC (Acqiris make) system has also been used to digitize 7-telescope data. Using Monte Carlo simulation studies, threshold energy (peak energy) of gamma rays incident vertically is calculated to be about 200 GeV [8]. The sensitivity of the telescope system from source like Crab nebula is $\frac{1.3\sigma}{\sqrt{T}}$ where T is observation time in hours and σ is statistical significance.

3 Observations and Data Analysis

The observations were carried out by pointing all telescopes in the source direction. For timing calibration of detectors data were collected with all telescopes stationary and pointing to zenith/fixed direction. In addition to Crab and Geminga pulsars, we have observed J0357+3206, J0633+0632 and J2055+2539 from Fermi pulsar catalog. Data were collected at a stretch, lasting for 30 minutes to 3 hours and covering hour angle range from -30 to +30 degree. The night sky condition is monitored throughout the observation using sky quality meter (SQM) and PMT. The observation log of sources after preliminary checks on data quality are given in Table-1.

Preliminary cuts and boundary limits on the data were applied for selection of events. The arrival times of the Cherenkov events were latched by a GPS -synchronized clock with an absolute time resolution of 1 μ s. The relative time of arrival of Cherenkov photons is fitted to a plane shower front and the arrival direction of the shower is estimated for each event [11]. The space angle (ψ) between the direction of arrival of the shower and the source direction, is obtained for each event. Figure-2 shows the typical space angle distributions for 40 minutes of data.

3.1 Periodic search

The TEMPO code¹ were used for the periodic analysis. In this procedure, the observed arrival times (t_{obs}) of recorded events from the isolated pulsar were converted to their barycentric position (t_{ssb}). The corrected barycentric times (t_{ssb}) were folded at the pulsar rotational frequency rela-

1. developed by the Princeton group

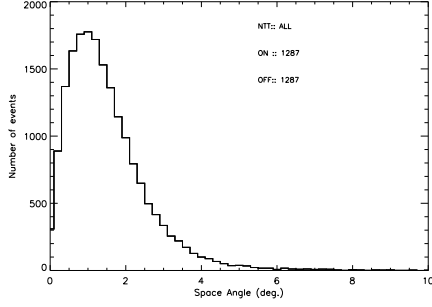


Figure 2: Space angle distribution

tive to epoch T_0 to get the phase ϕ as

$$\phi(T) = \phi(T_0) + f_0(T - T_0) + \frac{1}{2}\dot{f}(T - T_0)^2 + \frac{1}{6}\ddot{f}(T - T_0)^3$$

where $\phi(T_0)$ is the phase at epoch T_0 and is taken as a reference phase. The absolute phase of each event was obtained using TEMPO codes in “prediction mode” corresponding to the HAGAR site using contemporaneous pulsar parameters. In prediction or “tz” mode, reference phases are calculated over period of 4 hours (hour angle range) centered on the transit time the pulsars at Hanle observatory in steps of 20 min interval for each nights data. By using TEMPO polynomial coefficients and reference phase (ϕ_0), the absolute phase of an event at arrival time T is obtained by interpolation.

The monthly timing ephemeris of the Crab pulsar were extracted from Jodrel Bank crabtime data base [12]. The monthly timing ephemeris of the Geminga and three sources were derived from Fermi-Lat data. These details of pulsar data are given in table-2. PEPOCH in MJD is the epoch of period/frequency parameters. The reference data listed in column-2 has been extrapolated to the observation period of each source and monthly ephemerides were calculated and used in the phase analysis. The distribution of pulsar phases (Phasogram) is formed for each observation cycle with 20 phase bins and then added episodically. The phasograms of the Crab, Geminga, PSR J0357+3206, PSR J0633+0632 and PSR J2055+2539 events are shown in figure-3 to figure-7 for space angle ($\psi \leq 3.0$ degree). Any pulsed source will show up as peaks in the phasogram, as cosmic ray arrives randomly in time.

4 Results and discussion

Pulsed emission of radiation in the VHE band is expected at phases corresponding to the EGRET and Fermi-Lat detections. The phasogram for Crab and Geminga pulsars are divided into 4-regions, following the EGRET group [16], as shown in table-3. The number of events with phases within the P1 and P2 intervals constitute the signal events (N_{on}). The background events (N_{off}) are obtained by adding the

Table 2: Pulsar Ephemeris

PSR	Position (J2000) $f(s^{-1})$, $\dot{f}(s^{-2})$ and $\ddot{f}(s^{-3})$	Ref
Geminga	R.A. 06:33:54.2 Dec. 17:46:14.3 f : 4.21756706493 \dot{f} : -1.95250×10^{-13} \ddot{f} : 0 PEPOCH : 54800	[13]
J0357+3206	R.A. 03:57:52.4 Dec. 32:05:24.6 f : 2.25172229238 \dot{f} : -6.60925×10^{-14} \ddot{f} : -3.16061×10^{-23} PEPOCH : 54946	[3]
J0633+0632	R.A. 06:33:44.2 Dec. 06:32:34.9 f : 3.36252915875 \dot{f} : -8.99914×10^{-13} \ddot{f} : -2.41230×10^{-23} PEPOCH : 54945	[14]
J2055+2539	R.A. 20:55:48.9 Dec. 25:40:00.8 f : 3.12929095032 \dot{f} : -4.02192×10^{-14} \ddot{f} : 0 PEPOCH : 54900	[15]

Table 3: Pulsar phase intervals.

Source	P1	P2	Bridge	Background
Crab	0.95-0.05	0.35-0.45	0.05-0.35	0.45-0.95
Geminga	0.56-0.76	0.06-0.26	0.76-0.06	0.26-0.56
J0357+3206	0.85-0.25	-	-	0.25-0.85
J0633+0632	0.35-0.50	-	-	0.50-0.35
J2055+2539	0.16-0.50	-	-	0.50-0.16

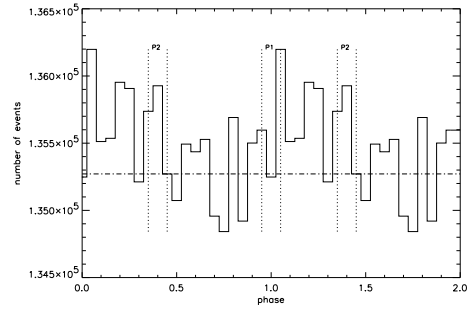


Figure 3: Phase histogram for Crab pulsar

number of events in the background region. The background events are normalized by multiplying the ratio of

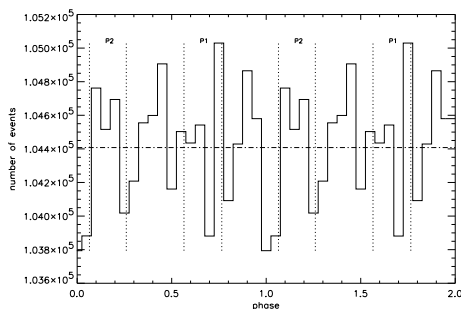


Figure 4: Phase histogram for Geminga pulsar

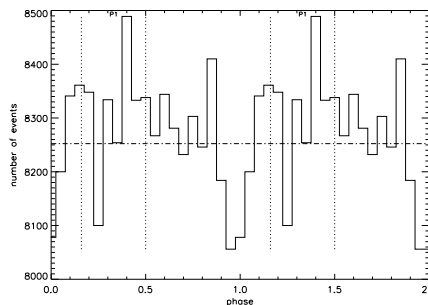


Figure 7: Phase histogram for PSR J2055+2539

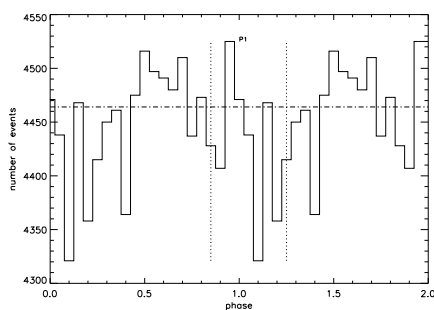


Figure 5: Phase histogram for PSR J0357+3206

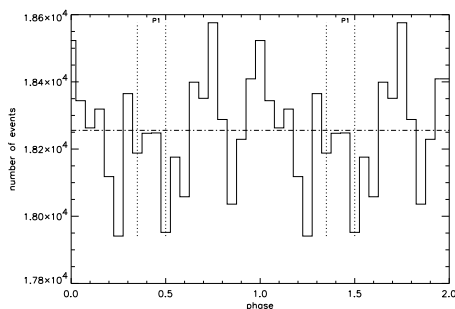


Figure 6: Phase histogram for PSR J0633+0632

phase ranges spanned by the pulse and non pulse region. The statistical significance (σ) of the excess signal were calculated according to method given by Li and Ma [17]. In the case of Fermi pulsars, phasograms are divided into 2-regions only, on pulse (P1) and background (off) region. The statistical significance of all listed pulsars are less than 1.6σ and do not show any evidence of pulsed emission of radiation for energies ≥ 205 GeV. The energy threshold corresponding to the average zenith angle (15 deg) of observations is 205 GeV and the collection area is 4.01×10^4 m². The time averaged gamma ray flux upper limit (3σ ul) obtained for sources are listed in table-4. The positive detection of Crab pulsar by MAGIC group for energies ≥ 25 GeV, the main pulse (P1) and inter-pulse (P2) have almost

Table 4: Upper limit on flux.

Source	Photon flux (3σ ul) (10^{-11} ph/cm ² /sec)
Crab	1.5
Geminga	3.6
PSR J0357+3206	14.1
PSR J0633+0632	3.7
PSR J2055+2539	10.1

equal peak amplitude and the ratio of P2/P1 increases with the energy as seen from the phasogram for events of energy ≥ 60 GeV. The FERMI result on Geminga pulsar shows that the ratio P2/P1 decreases as higher energy events are selected. The observation duration of PSR J2055+2539 is only 5.9 hours and less than 15 hours for other Fermi listed pulsars so we need more data to conclude about pulsed emission at VHE energies from these sources.

References

- [1] Hewish, A., Bell, S.J., et al., Nature,1968,**217**:709
- [2] Manchester, R. N., et al., ApJ, 1968, **129**:1993
- [3] Abdo, A. A. et al., ApJ, 2010, **187**:460-494
- [4] Daugherty, J. K, Harding, A.K., ApJ, 1996,**21**:251-254
- [5] Cheng,K.S., Ho,C., Ruderman,M.A., ApJ, 1986, **300**:500
- [6] Cheng, K. S., Ding, W. K. Y., ApJ, 1994,**431**:724
- [7] Muslimov and Harding, ApJ, 2004,**606**:1143
- [8] Chitnis, V. R., et al., Abstract ID:1089, OG 2.5, ICR-C2011
- [9] Aliu,E.,et al.,Science, 2008,**322**:1221-1224
- [10] Gothe, K.S., et al., preprint
- [11] Majumdar, P., et al., Astroparticle Physics, 2003 **18**:339
- [12] <http://www.jb.man.ac.uk/pulsar/crab.html>
- [13] Abdo, A. A. et al., ApJ, 2010, **720**:273-283
- [14] Ray, P.S., et al. 2011, ApJ, in press
- [15] Saz Parkinson, P.M. et al, ApJ, 2010, **725**:571
- [16] Fierro, J.M. et al., ApJ, 1998, **494**:734
- [17] Li, Ma, ApJ, 1983, **272**:317